Ortega-Ojeda, F.E, Torre-Roldán, M & García-Ruiz, C, 2017. Short wave infrared chemical imaging as future tool for analysing gunshot residues patterns in targets. Talanta (Oxford), 167, pp.227–235.

Available at https://doi.org/10.1016/j.talanta.2017.02.020

Short Wave Infrared Chemical Imaging as Future Tool for Analysing Gunshot Residues Patterns in Targets

F.E. Ortega-Ojeda, M. Torre Roldán, C. García-Ruiz

www.elsevier.com/locate/talanta

PII: S0039-9140(17)30224-2
DOI: http://dx.doi.org/10.1016/j.talanta.2017.02.020
Reference: TAL17296

To appear in: *Talanta*

Cite this article as: F.E. Ortega-Ojeda, M. Torre Roldán and C. García-Ruiz Short Wave Infrared Chemical Imaging as Future Tool for Analysing Gunshot Residues Patterns in Targets, *Talanta* http://dx.doi.org/10.1016/j.talanta.2017.02.020

Short Wave Infrared Chemical Imaging as Future Tool for Analysing Gunshot Residues Patterns in Targets[☆]

F.E. Ortega-Ojeda[*1], M. Torre Roldán[2], C. García-Ruiz[3]

Department of Analytical Chemistry, Physical Chemistry and Chemical Engineering, and University Institute of Research in Police Sciences (IUICP).

fernando.ortega@uah.es

mercedes.torre@uah.es

carmen.gruiz@uah.es;

[*]Corresponding author:

ABSTRACT

This work used chemical imaging in the short-wave infrared region for analysing gunshot residues (GSR) patterns in cotton fabric targets shot with conventional and non-toxic ammunition. It presents a non-destructive, non-toxic, highly visual and hiperspectral-based approach. The method was based on classical least squares regression, and was tested with the ammunition propellants and their standard components' spectra. The propellants' spectra were satisfactorily used (R^2 > 0.966, and CorrCoef > 0.982) for identifying the GSR irrespective of the type of ammunition used for the shooting. In a more versatile approach, nitrocellulose, the main component in the ammunition propellants, resulted an excellent standard for identifying GSR patterns (R^2 > 0.842, and CorrCoef > 0.908). In this case, the propellants' stabilizers (diphenilamine and centralite), and its nitrated derivatives as well as dinitrotoluene, showed also high spectral activity. Therefore, they could be recommended as complementary standards for confirming the GSR identification. These findings establish the proof of concept for a science-based evidence useful to support expert reports and final court rulings. This approach for obtaining GSR patterns can be an excellent alternative to the current and traditional chemical methods, which are based in presumptive and invasive colour tests.

[☆] Edificio Polivalente de Química, University of Alcalá, Ctra. Madrid-Barcelona Km. 33.6, 28871 Alcalá de Henares (Madrid), Spain

[1] Phone + 34 91 8854928

[2] Phone + 34 91 8854907

[3] Phone: + 34 91 8856431. Website: www.inquifor.com.

Keywords:

Gunshot residues; ammunitions; chemical image; hyperspectral image analysis; Classical Least Squares; Matlab.

1. Introduction

Gunshot residues (GSR) are particles produced when a firearm is discharged. They are composed of complex mixtures of inorganic and organic compounds that can be recovered from the crime scene and used as evidence during a court trial [1]. This is possible because they may adhere to the hands of the shutter, the victim clothes, the surface hit by the bullet, the firearm, and the environment in where the shooting took place [2-4]. The GSR composition results from the partial or total combustion of the ammunition primer, propellant gunpowder and metals from the projectile. Other compounds like grease, lubricants and metals from the firearm barrel may be also present [5].

Cartridges containing the projectile use smokeless gunpowders as propellants, which are essentially low explosives with a reaction rate slow enough to serve as projectiles' propellants. The bulk material in single-base smokeless gunpowders is mainly nitrocellulose. The propellant materials in double- and triple-base smokeless gunpowders may also include, but are not limited to, nitroglycerin, diglycol dinitrate, isomers of dinitrotoluene, nitroguanidine, and others [6-13] . Phthalates are added as plasticizers, and one or more stabilizers are always added to the gunpowder for preventing the spontaneous, exothermic and acid-catalysed decomposition of nitrocellulose, nitroglycerine, and similar nitric acid esters. Diphenylamine acts as a pure stabilizer that reacts with the nitrogen oxides formed by the slow nitrocellulose decomposition. As a consequence, the oxides are converted into their corresponding N-nitroso and nitro-derivates [14]. Other substances, such as methyl-centralite and ethyl-centralite, simplify the manufacturing of smokeless gunpowders because they can have both a stabilizing or gelatinizing effect [7]. The primer used to ignite the propellant in cartridges may contain inorganic compounds as nitrates, nitrites or heavy metals. In this respect, in conventional ammunition, any metal of the Pb, Sb, and Ba triade is accepted as specific marker of GSR.

Nowadays, there are non-tox ammunition (aka lead-free, heavy-metal-free, clean, or non-toxic-containing ammunition), which are being actively adopted all over the ammunition market [15]. They are slowly replacing the traditional heavy metal- or lead-containing ammunition. Interestingly, many type of re-manufactured/modified/re-loaded ammunition may include any type of commercially available primers. As a consequence, both lead containing and lead-free primers can be found in nowadays GSR [16]. This is a major concern for the forensic analysts who routinely use energy-dispersive X-ray spectroscopy (SEM-EDX) for the GSR identification based on their elemental composition. In order to achieve a valid GSR identification, the SEM-EDX method relays on detecting at least one compound of the triad Pb-Sb-Ba, which is available in the lead-containing ammunitions.

In recent years, Raman or Fourier transform infrared (FTIR) spectroscopy, have proved to be powerful techniques for acquiring the chemical signature of explosives, including those used as propellants [1, 17]. Raman spectroscopy has enabled the detection of lead sulphate and barium carbonate in the analysis of GSR [9]. This vibrational technique has proved to be very useful for identifying the organic components of GSR [9, 10]. In addition, it is an ideal technique when a non-destructive evidence analysis is required [2]. Accordingly, a Raman imaging system was recently used to study GSR particles in targets with and without blood contamination, as well as in police sample-collecting devices officially used for collecting GSR in suspect´s hands or clothing [18]. However, only few GSR particles were analysed at a time because the technique cannot be used on large areas as those exposed to GSR from real shootings. On the contrary, near-infrared (NIR), short-wave-infrared (SWIR), and mid-infrared (MIR) spectroscopy techniques, in the form of hyperspectral imaging (HSI) systems, are becoming very important because they can provide reliable chemical information from each space point regardless of the area (from mm^2 to Km^2) being analysed. Infrared HSI is a technology with key applications ranging from satellite based/airborne remote sensing and military target detection to industrial quality control and lab applications in food, medicine, biophysics, and others. However, HSI analysis has never been used for GSR analysis in spite of its suitability to analyse explosives like smokeless gunpowders [19, 20]. Therefore, the aim of this work was to stablish a proof of concept of using SWIR HSI chemical imaging for a non-destructive, non-toxic, rather quick, and highly visual chemical analysis of GSR patterns regardless of the type of ammunition (conventional and non-toxic) used for the shooting.

2. Material and methods

2.1. Samples and standards

All the analyses were performed on GSR obtained after firing guns with standard 9 mm ammunition on various types of targets. Both, lead ammunition known as S&B 9x19 08 (Sellier & Bellot AS, Vlašim, Czech Republic), and unleaded or "green" ammunition known as Geco SX 9x19 Sintox (RUAG, Berlin, Germany), were provided and shot by ballistic experts at the Spanish Police General Commissary. Due to patents and confidentiality reasons, the ammunitions composition is quite concealed, too varied, and not well-known. Nevertheless, Supplemental Table 1 collects the declared compositions of the S&B and Sintox ammunitions according to two official Safety Data Sheets and other references [5, 7, 13, 21-25]. In this study, the isolated propellants of both ammunitions were used as standards. Supplemental Table 2 shows some common compounds found in ammunitions. In this work, these compounds were also used as “pure” standards. Cellulose was obtained from Aldrich-Chemie (Steinheim, Germany), fabrics were acquired at local markets in Alcalá de Henares (Madrid, Spain), whereas other compounds were kindly provided by the Spanish Guardia Civil [26].

Each target (test sample, evidence-like) was made with a 40 x 40 cm cardboard base entirely covered with a piece of either white, black, or white-stamped cotton fabric. These fabrics were prewashed to eliminate potential contaminants. The different fabric colours were used to study whether there was any spectral difference and response due to the fabric or the dye in the fabric.

First, the targets were placed one by one in a clean shooting room at a 10 cm shooting distance. Then the firearms were fired with their corresponding lead-containing or lead-free ammunition. After every shot, and prior their HSI analysis, the targets were retrieved and stored in sealed bags to avoid any contamination.

2.2. Hyperspectral analysis

For the IR analysis of the targets, each one of those targets was taken out of its bag and placed on the analysis stage of the HSI system. Then, every target was exposed to the controlled IR diffused illumination of the HSI system. The standards spectra (all contributing species) were obtained by measuring them (so-called direct mode) directly from either the propellants or the pure compounds, not by estimating them from mixture spectra (so-called indirect mode). Hence, a reasonable amount of each granulated standard was deposited into the well of a microscope slide. Then, the slide was placed on the camera stage, illuminated and measured as the targets were. Dark and white references were also measured for every analysed sample. The different HSI analyses of both the targets and the standards were performed with a SWIR (1000 - 2500 nm) spectral camera (Specim, Spectral Imaging Ltd., Oulu, Finland) kindly provided by INFAIMON (Barcelona, Spain). The camera had a Mercury Cadmium Telluride (MCT) cryogenically cooled detector. All the data (HSI image) was gathered and then saved in binary hdr-raw ENVI format (Exelis, Boulder, Colorado, USA) with the in-built capture software of the HSI system.

A HSI image is a spatial and spectral representation of an object. Each pixel represents a physical point in the image, and contains the chemical information of the object at the pixel coordinates. This is because every pixel contains one spectrum. The global effect of a pixel/spectrum is seen when all other pixels/spectra are put together in a big image section or the whole image [27, 28]. This HSI images are nowadays huge 3D objects called hypercubes or cubes. The spectral resolution in these hypercubes is the number of individual wavelengths contained in each pixel, that is, the chemical information within the wavelength range (λ axis) for each pixel in the 2D digital image.

2.3. Data treatment

All data treatments were accomplished in a PC computer with an Intel Core-i7 processor, MS Windows (Redmond, WA, USA), and 16 GB of RAM. All the pre-treatments and analyses were performed with in-house algorithm sequences assisted by some freely-available HYPERTools, and Classification toolbox for Matlab [29, 30] functions programmed in Matlab (Matrix Laboratory, Natick, USA).

The large spectral data in a hypercube needs to be cleaned (pre-treated) in order to eliminate possible signal defects and artefacts (illumination defects, cosmic rays, dead pixels and wavelengths), high noise levels, baseline drifts or offsets, non-informative image regions, etc., while improving its quality [28]. First, and regardless of the type of hypercubes (targets and standards), the original illumination artefacts of all cubes was minimised using their corresponding dark and white references [31]:

Normalised Image = (Measured Image – Dark Ref.) / (White Ref. – Dark Ref.)

Afterwards, several functions offered by HYPERTools were executed for pre-processing the cubes. This way, both the dead wavelengths and pixels were eliminated with their appropriate filters. Next, each HSI image was spatially cropped for discarding most of the useless peripheral image areas, like non-relevant objects (surfaces, areas, etc.) outside the standard particles or the shot target. Then, the images underwent a masking step by graphical Principal Component Analysis (PCA), using the functions and methods also available in HYPERTools. A mask is a binary design/object/layer/pattern that adopts any specific shape arranged to further isolate the regions of interest (ROI) or image portions containing only the actual target or standards' signal, without altering the actual image being masked. In these cases, by means of PC1, all heavily shadowed, overexposed, and remaining non-ROI areas highlighted by the masks were left out of the images. Only a small, representative well-illuminated part of each standard was kept for the spectra extraction, thus guarantying the availability of the corresponding pure spectra. The target (evidence) images did not receive any extensive cropping or further masking, in order to keep as much test (evidence-like) area as possible for the subsequent matching/resolution step. This was opted despite that such a large amount of target pixels was known to immensely increase the matching/computing time. Nevertheless, the target samples had to resemble any medium size real case evidence samples.

Finally, in order to obtain the lowest prediction error and the best signal-to-noise response with minimal spectra modification, all newly cleaned standard and target images underwent further spectral pre-processing: i) baseline correction (second-degree polynomial fitting and subtraction), ii) normalisation (Standard Normal Variate, SNV), and iii) smoothing (Savitzky-Golay filtering) [27, 28]. The smoothing used a symmetrical window value of 5, and a second-degree polynomial. All these mathematical treatments are well-known for providing very good results while being easy to apply to IR and other spectroscopy data [19, 28, 32-35].

After the main spectral pre-treatment, the whole process was handled in two large phases, to uncover the chemical information buried in the spectra data: a) The calibration and Classical Least Squares (aka K-matrix method, CLS), model creation using the pre-isolated standards' spectra collection (both standards and propellant spectra); and b) The matching of the target (shot) samples against the previously created models.

2.4. Calibration

Each standard or ammunition propellant type was designated as the calibration class (family, type, or group) working as an internal library of well-known compounds possibly present in the evidence sample. For assembling the calibration set, at least 5 spectra from every masked standard image were randomly selected covering a random mesh-like region on the standard's ROI surface. From those spectra, the most common spectrum was chosen as the pure standard spectrum. Likewise, 10 spectra from each ammunition propellant image were obtained randomly and directly from the ammunition image. This was decided so because the propellant powder was a dry mixture of components, hence the obtained spectra corresponded to different unlabelled compounds. From that spectra assembly, only those which

generated better ammunition propellant differentiation in a fabric were chosen based on their intensity differences.

Since the calibration images were different from the evidence (target) images, the library spectra were never used again for the actual matching/resolution steps, thus avoiding the "double dipping" mistake. Hence, the entire library combining the propellants and pure compounds spectra contained 38 known standard spectra.

After assembling the calibration set, the corresponding global CLS regression models were created applying no-negativity constraints. The initial spectra for the CLS analyses, were taken from the calibration set.

2.5. Validation

The prediction power of the CLS models or the measure of fit, was calculated using the squared correlation coefficient (R^2, aka coefficient of determination, or the fraction of the variability in the response that is accounted for by the model)[36]. Besides, the goodness of fit was also assessed by calculating the lack of fit of the model (LOF)[37, 38], and the Pearson Correlation Coefficients of any CLS-predicted spectrum against its well-known counterpart [32]. The significance level used for these tests was always 0.05.

2.6. Matching

All the pre-treated spectra from each target (evidence) image were compared against all the pre-treated spectra present in the calibration set using the CLS (aka K-matrix method) models that designates the spectral response acting as the dependent variable in the Beer-Lambert's law equation [39]. This very effective regression tool requires that all the components of the system must be known and measurable to discern the individual contributions to the mixture response [39-41]. The procedure renders individual coloured chemical maps locating every detectable standard or propellant spectrum on the image. These relative (aka pseudo-concentration or concentration) maps are equivalent to the estimated weight of each component (standard or propellant) in the test sample. The algorithms were set to show only those chemical maps having a threshold of relative weight over 10 %. Furthermore, the CLS algorithm also estimated the relative density of each standard in the target chemical map by counting the number of standard pixels found in the entire image with respect to 100 existing pixels in that image. In this case, a value close to zero would indicate the absence of a particular standard, while a value near 100 (or 1 in the 0-1 scale) would imply the total presence of that standard in the target. Similarly, the colours in the chemical map represent the intensity and location of each matched standard, ranging from 0 to 1 (or 0 to 100, in a percentage scale). This way, blue is the smallest value, indicating the absence of the matched standard in the image, whereas red is the highest value, showing a total presence of the matched standard. Note that the two parameters (relative weight and density) are contributory, i.e., they are not cumulative, thus, the total value might slightly exceed the top limit.

It is worth stressing that all the large target test images this study worked with were cropped down to a size of 512x318x238 (310001664 bytes). Despite that, the evidence images were still huge, containing 162816 spectra. This size typically surpasses the usual computational power of common computers. Therefore, the algorithm had to be flexible enough to handle such amount of data and processing load.

3. Results and discussion

To develop a SWIR-HSI chemical imaging method was essential for studying different multivariate data analysis (MVA) techniques. There are many of such relevant and well-established MVA procedures useful to uncover the chemical information buried in the spectral data. Examples of these are Principal Component Analysis, Classical Least Squares, Projection to Latent Structures, Multivariate Curve Resolution - Alternating Least Squares, Fuzzy C-Means, etc. In this work, CLS was chosen for being a very effective regression tool for the analyses of SWIR images of GSR patterns in cotton fabric targets shot with conventional and non-toxic ammunition. The main requirement for the use of CLS with this aim, as in other similar chemical imaging applications within pharmaceutical or food science [27, 32, 34, 35, 42], were the knowledge of the pure analytes spectra and their guaranteed orthogonality. Therefore, CLS could be safely applied to create regression models which provide a rather easy, simple, and reliable approximation of the analytes concentration within each pixel.

Moreover, CLS was chosen because its speed. When using the three fabric's library spectra as the initial estimations/standards, the CLS script using the light HYPERTools CLS functions processed those evidence images in about 11 – 16 min. When using 21 standard spectra from the library, the CLS algorithm took about 8 – 16 min on the same target sample. Therefore, the CLS algorithm showed rather good speed.

Hence, the first analysis method developed on the basis of SWIR HSI chemical imaging focused on detecting the differences between various fabrics potentially occurring as supports in real GSR cases. Accordingly, three different targets made with white, black, or white-stamped fabrics, shot at 10 cm with either S&B and Sintox ammunition, were studied.

All targets were matched against the standards' spectra of white, black, or white-stamped cotton fabrics. Figure 1 represents the CLS results showing the comparison of the chemical images of white-cotton-fabric targets shot at 10 cm with either S&B (top row) or Sintox (middle row) ammunition. The standard´s spectra used for the matching corresponded to the white, black, or white-stamped cotton fabrics (bottom row). It can be seen that regardless of the ammunition shot on the white-cotton-fabric target, the only standard detected with high relative weight and density values corresponded to the white-cotton-fabric material. However, some traces of the stamped-cotton-fabric were detected on the white-cotton-fabric. This occurred probably because both fabrics (white- and stamped-cotton) were white-cotton-based, and thus their spectra were very similar even despite the stamping process. That is, the stamping dye did not properly hide the spectrum of the white-cotton fibres underneath, which is the case in the black-cotton-fabric. Interestingly, the areas around the shot hole in the black-cotton-fabric did show some presence of the white-cotton-fabric spectrum. In this case, it looked like the high-speed

bullet passed scratching somehow the fabric dye, thus exposing some of the white-cotton-fabric material that it was originally made off.

Table 1 shows the statistical parameters calculated to validate the CLS analyses on the targets made with the three cotton fabrics, and shot at 10 cm with both S&B or Sintox ammunitions. These three statistic parameters useful to show the goodness-of-fit of the CLS model are: LOF, R^2, and the Pearson Correlation Coefficient with its standard deviation. In the case of the white-cotton targets, the LOF values (from 9.40 to 25.00) for the CLS model may evidence some noise in the spectra [36, 43, 44], nevertheless, the high prediction power of the CLS models was shown with high squared correlation coefficients ($R^2 > 0.94$). Furthermore, the mean values of the Pearson Correlation Coefficients calculated for the original target white-cotton-fabric spectrum vs. at least 500 white-cotton calculated spectra were also high (CorrCoef > 0.965). Similar results were also calculated for the black- and pattern-cotton-fabrics. All the p-values were p <<< 0.05. Thus, the calculated CLS models were highly valid for estimating both the relative weight and density maps shown in Figure 1.

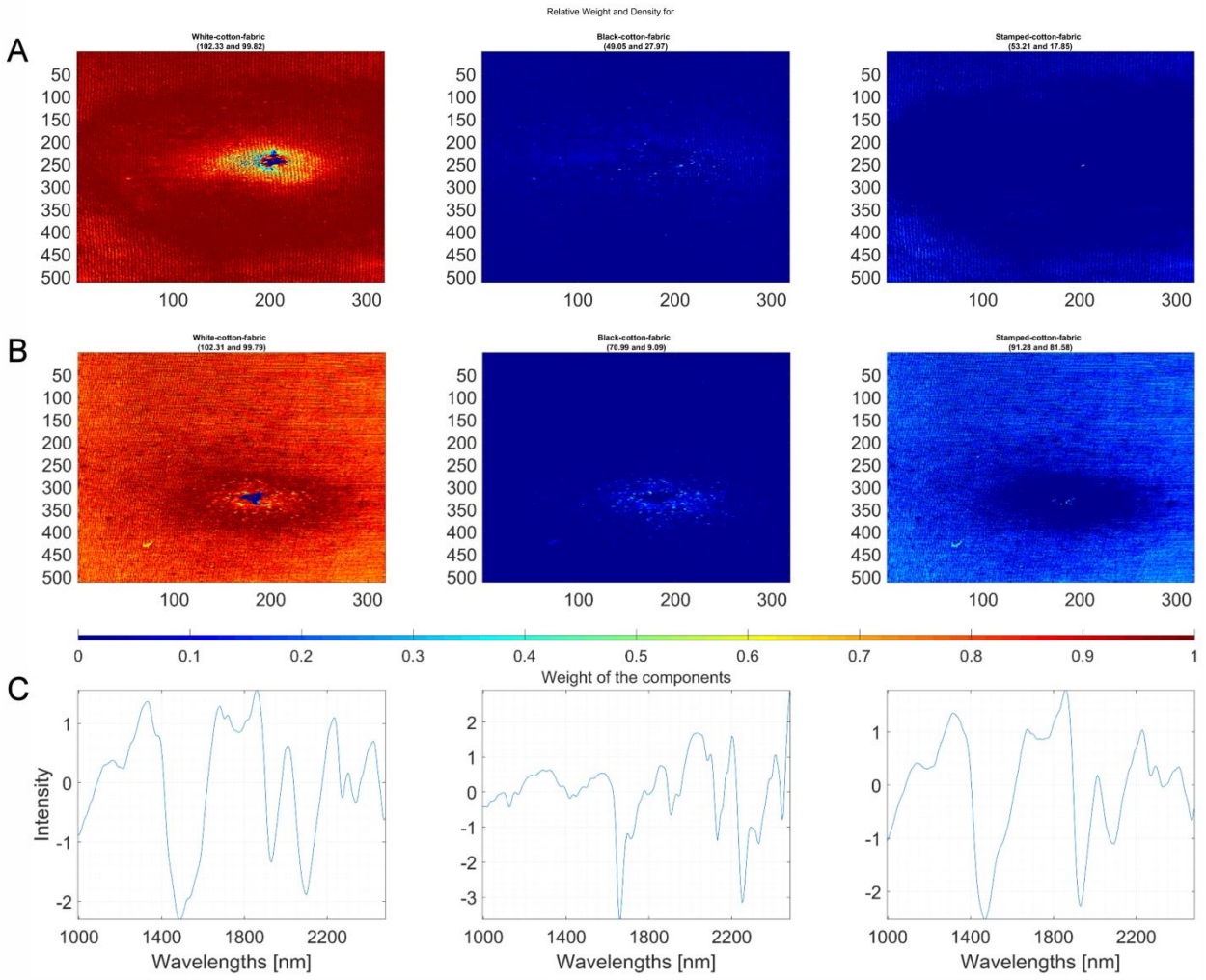

Figure 1. CLS results showing the GSR patterns of (A) S&B and (B) Sintox ammunition shot on white-cotton-fabric targets at 10 cm. Each target, which is the same in all horizontal images, was matched against the white, black or white-stamped cotton

fabrics working as standards' spectra, placed at the bottom row (C). Relative weight and density are the quantitative values indicated inside parenthesis.

As a result of these findings, and in order to establish the proof-of-concept for a fast, easy, reliable, and distinctive way for obtaining GSR patterns by SWR-HSI, only both white- and black-cotton-fabrics were used as targets in the subsequent studies. Hence, the next step was to study the GSR patterns of both lead-containing (S&B) and non-tox (Sintox) ammunitions fired at 10 cm distance on the white- and black-cotton-fabrics. As an initial approach, the matching was performed using their own ammunition propellant as standards for the identification of GSR in targets.

Table 1. Statistical parameters calculated to validate the CLS analyses on the targets made with white-, black, and pattern-cotton fabrics, and shot at 10 cm with either S&B or Sintox ammunitions.

Target	Ammunition	CLS		
		LOF	R^2	Pearson Correlation Coefficients*
White-cotton	S&B	19.700	0.960	0.999 ± 0.001
	Sintox	9.400	0.990	0.997 ± 0.002
Black-cotton	S&B	25.000	0.940	0.965 ± 0.082
	Sintox	13.100	0.980	0.992 ± 0.014
Stamped-cotton	S&B	12.240	0.990	0.993 ± 0.012

LOF = Lack of fit of the CLS model.
* Calculated for the original target white-cotton-fabric spectrum vs. at least 500 white-cotton calculated spectra.
p <<< 0.05.

Figure 2 represents the CLS results showing the relative weight and density chemical maps of white- and black-cotton fabrics shot at 10 cm with either S&B or Sintox ammunitions. The targets were matched against the spectrum of the target's fabric and the 20 spectra of both propellants. Figures 2A and 2C represent the targets shot with the S&B ammunition, while Figures 2B and 2D show the targets shot with the Sintox ammunition. It can be seen, as was the case in Figure 1, that each fabric standard was properly detected in its corresponding target. Hereafter, the strongest detected standards from both S&B and Sintox propellants occurred in the targets shot with the S&B ammunition (Figures 2A and 2C). Here the GSR patterns observed seemed to be bigger than the patterns observed in the targets shot with the Sintox ammunition. It is important to mention that every propellant's chemical map shown here resulted from the accumulation of all the ten individual sub-maps created from each propellant's spectrum (Supplemental Figure 1, left). In other words, the chemical heterogeneity of each powdered propellant rendered ten individual chemical maps. This way, the entire matching produced 21 chemical sub-maps belonging to the corresponding cotton-fabric and 20 ammunition standards. Such number of chemical maps does not properly fit in a comprehensible single picture. Hence, all the individual chemical maps pertaining to the same propellant were added to create one single accumulated chemical map, which was also more self-explanatory and visually conclusive. Although shooting with the Sintox ammunition did not leave large GSR in both fabrics, the propellants' presence was indeed detected with reasonable intensities in both targets (Figures 2B and 2D). Regarding the black-cotton fabric, it seemed that at least the black dye appeared to hinder somehow the detection of both propellants. Nevertheless, it is noteworthy to stress that all the GSR were anyway detected regardless of

the ammunition and fabric used in the shooting. This is a relevant result and an advantage of the SWIR-HSI method proposed in this study when compared to the routinely used SEM-EDX, which results in false negatives when analysing lead-free residues. This limitation is due to the lack of Pb and other heavy metals in those samples. Such residues were here successfully identified as GSR when using SWIR-HSI and the standards' spectra of the whole powdered propellant.

Table 2 shows the statistical parameters calculated to evaluate the CLS analyses on the targets made with white- and black cotton fabrics, shot at 10 cm with both S&B or Sintox ammunitions, but matched only against the corresponding cotton fabric and the 20 propellant spectra. In this entire propellant-based approach, when considering the case of the white-cotton targets (Figures 2A and 2B), the values of the LOF (from 8.30 to 18.52) for the CLS models could indicate again some noise in the spectra. Nevertheless, the high values of the squared correlation coefficients (R^2 > 0.966) for the CLS models showed again high prediction power. In addition, the models showed also good mean values for the Pearson Correlation Coefficients (CorrCoef > 0.982) calculated for the original target white-cotton-fabric spectra vs. all the propellants' calculated spectra. Similar values were also obtained for the black-cotton fabric. All the p-values were p <<< 0.05. Hence, the calculated CLS models were highly valid for estimating both the relative weight and density maps shown in Figure 2.

Table 2. Statistical parameters calculated to evaluate the CLS analyses on the targets made with the white- and black cotton fabrics, shot at 10 cm with both S&B or Sintox ammunitions, but matched against the corresponding cotton fabric and the 20 propellant spectra.

Target	Shot Ammunition	Matching STDs	CLS		
			LOF	R^2	Pearson Correlation Coefficients*
White-cotton	S&B	White-cotton	13.00	0.980	0.992 ± 0.021
		S&B			0.989 ± 0.025
		Sintox			0.990 ± 0.025
	Sintox	White-cotton	8.30	0.990	0.997 ± 0.003
		S&B			0.997 ± 0.004
		Sintox			0.997 ± 0.003
Black-cotton	S&B	Black-cotton	18.52	0.966	0.982 ± 0.035
		S&B			0.982 ± 0.036
		Sintox			0.982 ± 0.036
	Sintox	Black-cotton	10.00	0.990	0.995 ± 0.007
		S&B			0.995 ± 0.007
		Sintox			0.995 ± 0.007

LOF = Lack of fit of the CLs model.
* Calculated for the original target white-cotton-fabric spectra vs. all the propellants' calculated spectra.
p <<< 0.05.

Although this approach provided satisfactory results, not all forensic laboratories have a reasonable large sample library containing several types of ammunition propellants to be used as HSI standards. Consequently, a more versatile method based on the use of standards from available commercial ammunition components (Supplemental Table 2) was also tested for obtaining reliable SWIR-HSI chemical images of GSR patterns.

Figure 3 shows the relative weight and density chemical maps of white- and black-cotton fabrics shot at 10 cm with either S&B or Sintox ammunitions. The targets were matched against the spectra of the standards shown in Supplemental Table 2. Figures 3A and 3B show the white-cotton-fabric targets, whilst Figures 3C and 3D show the black-cotton-fabric targets. Figures 3A and 3C represent the targets shot with the S&B ammunition, while Figures 3B and 3D show the targets shot with the Sintox ammunition.

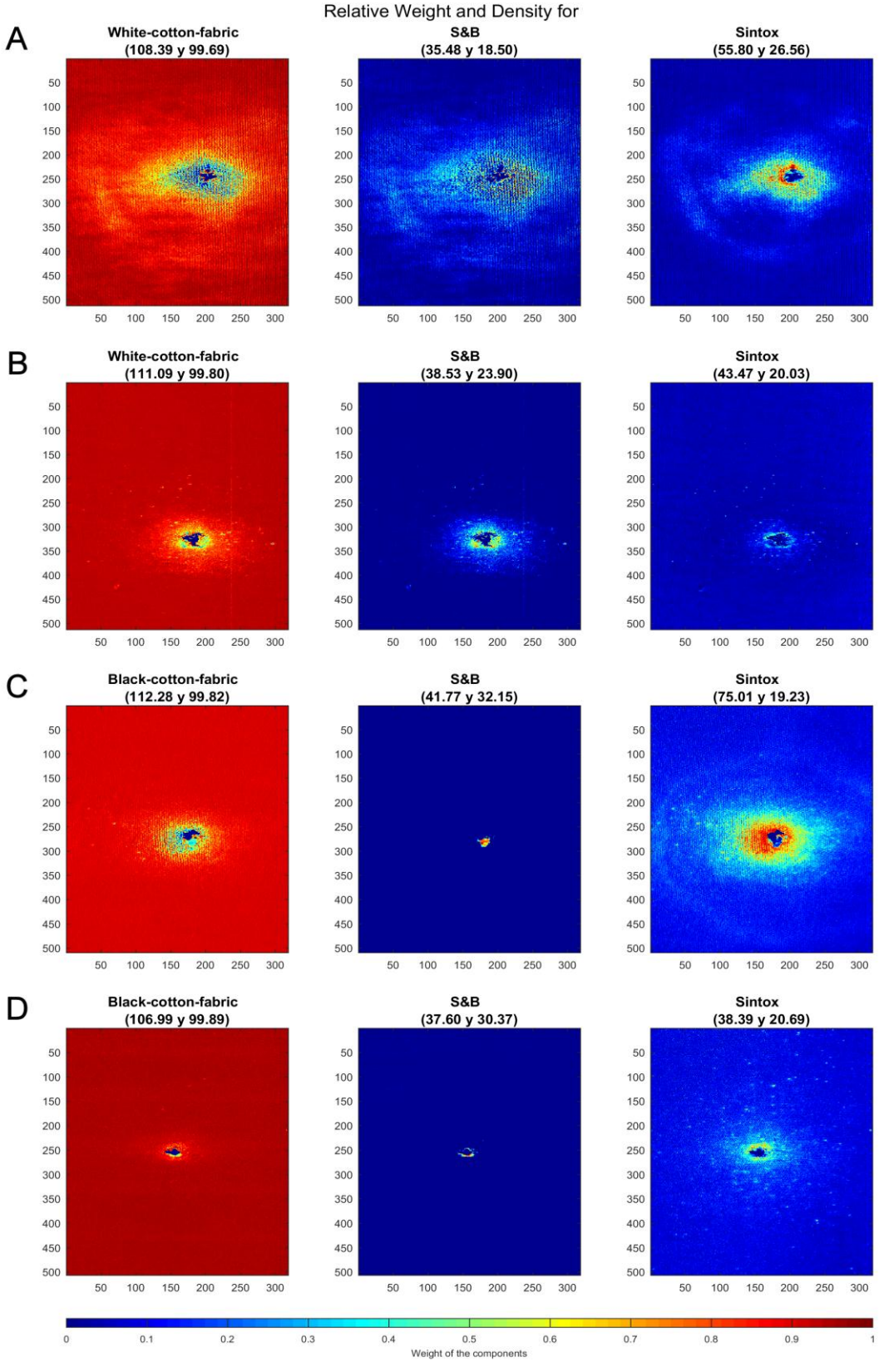

Figure 2 CLS results showing the GSR patterns in white- and black-cotton fabrics shot at 10 cm with either S&B or Sintox ammunitions when targets were matched against both propellants' spectra and the corresponding target's spectrum. A) White-cotton-fabric shot with S&B; B) White-cotton-fabric shot with Sintox; C) Black-cotton-fabric shot with S&B; and D) Black-cotton-fabric shot with Sintox. Relative weight and density are the quantitative values indicated into parenthesis.

As occurred in the ammunition propellant-approach, the strongest spectral signals were detected in the targets shot with the S&B ammunition (Figures 3A and 3C). Contrarily, the material deposited by shooting the Sintox ammunition produced smaller GSR patterns in both fabric types (Figures 3B and 3D). Again, it was possible to infer that the black-cotton fabric might have hampered somewhat the detection of the calibration standards. Nonetheless, all the GSR patterns were detected regardless of the ammunition and fabric used in the shooting.

The strongest signals found in all targets belonged to nitrocellulose (Supplemental Figure 1, right). This is not surprising since nitrocellulose is the largest propellant's component in both S&B and Sintox ammunitions (ca. 70, and 73 to 85 %, respectively, according to Supplemental Table 1). However, it is very interesting to see that the detection of all the other strongest standards found also seemed to depend on the type of cotton-fabric in the targets. Those components were mainly diphenylamine, nitroguanidine, 4-nitro-ethyl-centralite, and 2,6-dinitrotoluene (Supplemental Figure 1, right). These findings were striking, albeit are very important because such standards can be used to focus exploratory searches towards GSR, or to confirm their presence. With regard to the white-cotton-fabric chemical maps, the stabiliser diphenylamine and various of its derivatives (maps not shown) were expected since they are mixed within the propellants, and are commonly found in GSR [8, 45]. Nitroguanidine is reported as part of the primers in several lead-free ammunition [9-11]. However, despite that this component is reported as not so common in single- and double-base ammunition, it resulted fairly curious to indeed find it in the GSR of the S&B ammunition. These results can be accepted because many commercial propellants may be the mixed products of recycling other military-grade propellants.

Regarding the black-cotton-fabric chemical maps shot with the S&B ammunition, finding 4-nitro-ethyl-centralite and 2,6-dinitrotoluene (Supplemental Figure 1, right) is quite anticipated as centralite and dinitrotoluene are already reported as components of that ammunition. However, as centralite was not declared in the Sintox ammunition, finding its nitrated derivatives was surprising. Nonetheless, these type of GSR have been already reported in lead-free ammunitions [45], and in fact, they might be already part of them as well as other diphenylurea-based compounds [7, 12]. Consequently, the use of nitrocellulose and dinitrotoluene as standards in the SWIR-HSI analysis may also provide reliable information for the identification of GSR.

Table 3 shows the statistical parameters calculated to evaluate the CLS analyses on the targets made with white- and black cotton fabrics, shot at 10 cm with S&B or Sintox ammunitions, but matched against the individual pure spectra reported as part of the S&B and Sintox ammunitions (Figure 3).

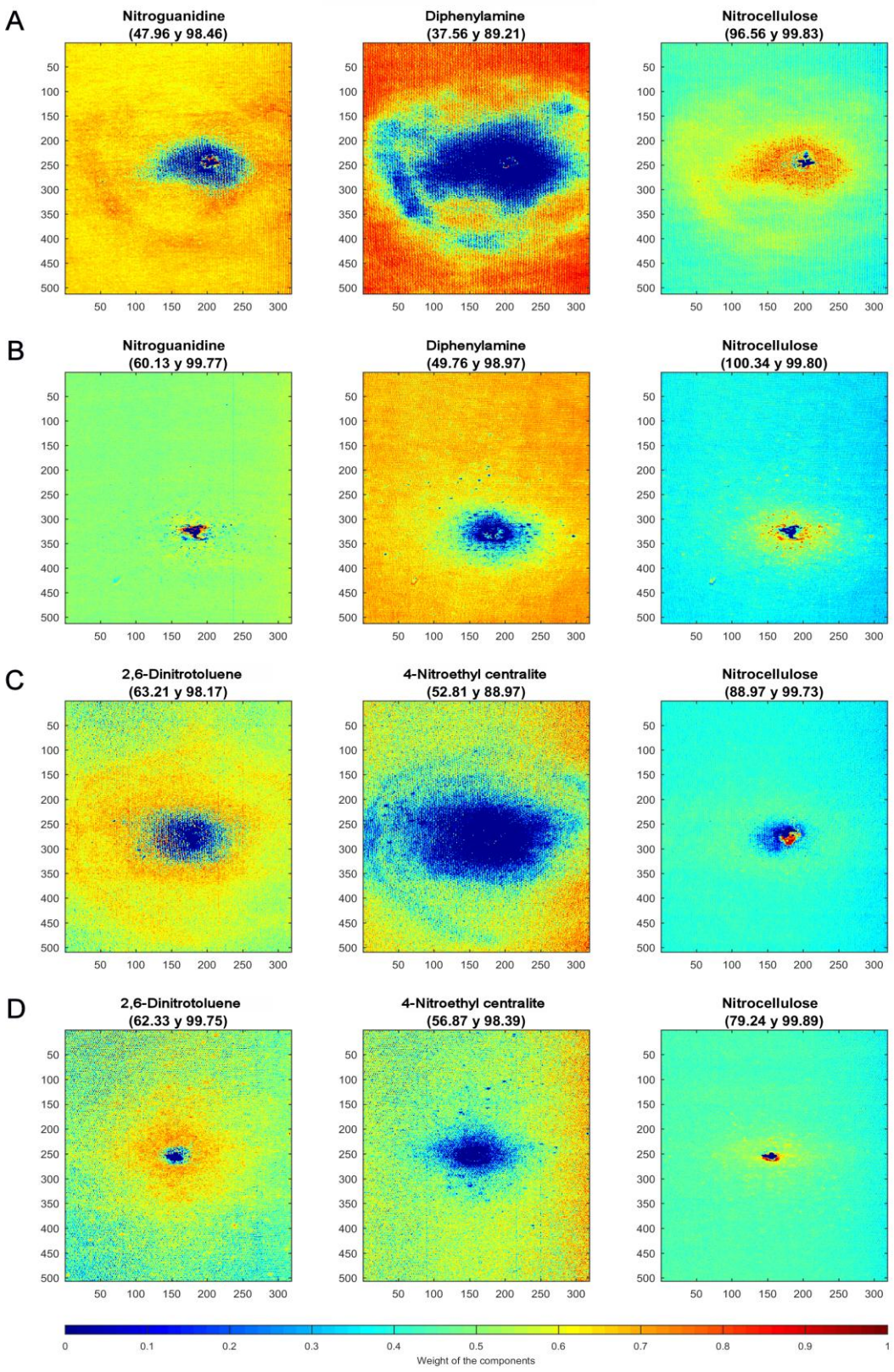

Figure 3. CLS results showing the GSR patterns in white- and black-cotton fabrics shot at 10 cm with either S&B or Sintox ammunitions when targets were matched against the spectra of the pure standards. The cotton-fabrics, cellulose, and the ammunition standards were kept out in order to keep the images as uncrowded as possible. A) White-cotton-fabric shot with S&B; B) White-cotton-fabric shot with Sintox; C) Black-cotton-fabric shot with S&B; and D) Black-cotton-fabric shot with Sintox. Relative weight and density are the quantitative values indicated into parenthesis.

When considering the case of the white-cotton targets (Figures 3A and 2B), the LOF values (from 21.27 to 39.79) of the CLS models may evidence noise in the spectra. Still, the squared correlation coefficients values (R^2 > 0.842) for the CLS models presented again rather good prediction power. Moreover, the models showed also good mean values for the Pearson Correlation Coefficients (CorrCoef > 0.908) calculated for the original target white-cotton-fabric spectra vs. all the calculated spectra of the standards (Supplemental Table 2). Similar values were also calculated for the black-cotton fabric. All the p-values were p <<< 0.05. Therefore, the calculated CLS models were valid for estimating both the relative weight and density maps shown in Figure 3.

Table 3. Statistical parameters calculated to evaluate the CLS analyses on the targets made with the white- and black cotton fabrics, shot at 10 cm with both S&B or Sintox ammunitions, but matched against the individual pure spectra reported as part of the S&B and Sintox ammunitions (Table 2).

			CLS		
Target	Shot Ammunition	Matching STDs	LOF	R^2	Pearson Correlation Coefficients*
White-cotton	S&B	'Nitroguanidine'	39.790	0.842	0.908 ± 0.110
		'Diphenylamine'			0.912 ± 0.108
		'Nitrocellulose'			0.917 ± 0.045
	Sintox	'Nitroguanidine'	39.310	0.845	0.920 ± 0.010
		'Diphenylamine'			0.920 ± 0.010
		'Nitrocellulose'			0.920 ± 0.011
Black-cotton	S&B	'2,6-Dinitrotoluene'	31.320	0.902	0.954 ± 0.050
		'4-Nitro-Etilcentralite'			0.966 ± 0.014
		'Nitrocellulose'			0.948 ± 0.077
	Sintox	'2,6-Dinitrotoluene'	21.270	0.955	0.978 ± 0.007
		'4-Nitro-Etilcentralite'			0.978 ± 0.004
		'Nitrocellulose'			0.978 ± 0.007

LOF = Lack of fit of the CLs model.
* Calculated for the original target white-cotton-fabric spectrum vs. all the standards calculated spectra (Supplemental Table 2).
p <<< 0.05.

4. Conclusions

This work proves that chemical imaging in the NIR region (1000 - 2500 nm) is an important future tool for a non-destructive, non-toxic, highly visual and fast analysis of GSR patterns in targets.

Although the propellant spectra were successfully used for identifying the GSR regardless of the type of ammunition employed for the shooting (conventional or non-tox ammunition), the use of nitrocellulose as standard makes this approach more versatile for laboratories. This is because nitrocellulose is the largest component in the ammunition's propellant, and so it was easily detected in the chemical images. This standard-based approach can be complemented by using some of the common stabilisers found in

the ammunition's propellant. Compounds like diphenylamine and/or centralite, and its nitrated derivatives, and dinitrotoluene, show high spectral activity, and can well be used as complementary standards for identifying GSR.

The propellant´s component standard-based approach presents the added value of its applicability regardless of the type of ammunition employed for the shooting. This is because it focuses on the propellant components, which are mainly organic compounds.

These findings establish the proof of concept for a science-based evidence useful to support expert reports and final court rulings. This that can be an excellent alternative to the current and traditional chemical methods for obtaining gunshot patterns, which are based in presumptive and invasive colour tests.

Acknowledgements

The authors would like to acknowledge the financial support of Ministerio de Economía y Competitividad for funding the project CTQ-2014-58688-R. We also thank Dr. Carolina López and Jordi Alaman (INFAIMON, Barcelona) for letting us use the HSI system. We also thank Dr. María López, Dr. Mª Ángeles Fernández de la Ossa, and Erika Herranz for helping in this study during its shooting, measuring, and screening/exploring stages. We would like to thank the Spanish Police General Commissary for providing and shooting the ammunition used in this study. We want to thank the Servicio de Criminalística de la Guardia Civil for helping with some ammunition information and standards.

References

[1] J. Bueno, V. Sikirzhytski, I. Lednev, K., Raman Spectroscopic Analysis of Gunshot Residue Offering Great Potential for Caliber Differentiation, Analytical Chemistry 84(10) (2012) 4334-4339.
[2] M. López-López, J.J. Delgado, C. García-Ruiz, Ammunition Identification by Means of the Organic Analysis of Gunshot Residues Using Raman Spectroscopy, Analytical Chemistry 84(8) (2012) 3581-3585.
[3] J. Bueno, I. Lednev, K. , Attenuated Total Reflectance-FT-IR Imaging for Rapid and Automated Detection of Gunshot Residue, Analytical Chemistry 86(7) (2014) 3389-3396.
[4] J. Bueno, V. Sikirzhytski, I. Lednev, K., Attenuated Total Reflectance-FT-IR Spectroscopy for Gunshot Residue Analysis: Potential for Ammunition Determination, Analytical Chemistry 85(15) (2013) 7287-7294.
[5] E. Goudsmits, G.P. Sharples, J.W. Birkett, Recent trends in organic gunshot residue analysis, Trends in Analytical Chemistry 74 (2015) 46–57.
[6] D.M. Northrop, W.A. MacCrehan, Smokeless powder residue analysis by capillary electrophoresis. National Institute of Justice Report 600-91, in: U.S.D.o. Justice (Ed.) National Institute of Justice, 1997, pp. 1-15.
[7] F.S. Romolo, Organic Gunshot Residue from Lead-Free Ammunition, INSTITUT DE POLICE SCIENTIFIQUE. ECOLE DES SCIENCES CRIMINELLES, L'Université de Lausanne, Lausanne, 2004, p. 235.

[8] N.G.I. Reboleira, Caracterização Química de Resíduos de Pólvora na Identificação de Munições, Faculdade de Ciências. Departamento de Química e Bioquímica, Universidade de Lisboa, Lisboa, Portugal, 2013, p. 104.
[9] J. Erickson, J.L. Sandstrom, G. Johnston, N. Norris, P. Braun, R. Blau, L.S. Liu, Non-toxic percussion primers and methods of preparing the same, Google Patents, 2013.
[10] J. Erickson, J.L. Sandstrom, G. Johnston, N. Norris, P. Braun, R. Blau, L.S. Liu, R.H. Newell, Non-toxic percussion primers and methods of preparing the same, Google Patents, 2013.
[11] J. Sandstrom, A.A. Quinn, J. Erickson, Non-toxic, heavy-metal free sensitized explosive percussion primers and methods of preparing the same, Google Patents, 2012.
[12] R. Meyer, J. Köhler, A. Homburg, Explosives, Sixth ed., Wiley-VCH & Co. KGaA, Weinheim2007.
[13] S. Fordham, Manufacture of Propellants, High Explosives and Propellants, Pergamon Press1980, pp. 169-177.
[14] J.B. Apatoff, G. Norwitz, Role of Diphenylamine as a Stabilizer in Propellants; Analytical Chemistry of Diphenylamine in Propellants. A Survey Report., in: U.S.A.A. COMMAND (Ed.) U.S. ARMY ARMAMENT COMMAND, FRANKFORD ARSENAL, 1973, p. 47.
[15] B.J. Heard, Ammunition, Handbook of Firearms and Ballistics. Examining and Interpreting Forensic Evidence, Wiley-Blackwell. John Wiley & Sons2008, pp. 43-99.
[16] The Scientific Working Group for Gunshot Residue - SWGGSR, Guide for Primer Gunshot Residue Analysis by Scanning Electron Microscopy/Energy Dispersive X-Ray Spectrometry. 11-29-11, in: N.I.f.J. (NIJ) (Ed.) The Scientific Working Group for Gunshot Residue (SWGGSR), 2011, pp. 1-100.
[17] M. López-López, C. García-Ruiz, Infrared and Raman spectroscopy techniques applied to identification of explosives, TrAC Trends in Analytical Chemistry 54 (2014) 36-44.
[18] M. López-López, M.Á. Fernandez de la Ossa, C. García-Ruiz, Fast Analysis of Complete Macroscopic Gunshot Residues on Substrates Using Raman Imaging, Appl Spectrosc. (1943-3530 (Electronic)) (2015).
[19] M.Á. Fernández de la Ossa, C. García-Ruiz, J.M. Amigo, Detection of residues from explosive manipulation by near infrared hyperspectral imaging: a promising forensic tool, Forensic Science International 242 (2014) 228–235.
[20] M.Á. Fernández de la Ossa, C. García-Ruiz, J.M. Amigo, Near infrared spectral imaging for the analysis of dynamite residues on human handprints, Talanta 130 (2014) 315–321.
[21] Sellier & Bellot, Safety Data Sheet. Pursuant to Directive 91/155/EEC. CENTRE-FIRE CARTRIDGES, in: S. Bellot (Ed.) Rifle, pistol, and revolver centre-fire cartridges, Vlašim, Czech Republic, 2009, p. 6.
[22] Sellier & Bellot, Material Safety Data Sheet according to Regulation (EC) Nº 1907/2006, in: S. Bellot (Ed.) Shotgun shells, Czech Republic, 2014, p. 10.
[23] RUAG Aerospace Defence Technology, Material Safety Data Sheet, Rimfire cartridges, RUAG Ammotec Gmbh, Fürth, Germany, 2005, p. 9.
[24] RUAG Aerospace Defence Technology, EC- Safety Data Sheet, Cartridges for bolt stunners Cal. 6.8/15 SINTOX (Schermer), RUAG Ammotec Gmbh, Fürth, Germany, 2007, p. 5.
[25] N. Kubota, Energetics of Propellants and Explosives, Propellants and Explosives. Thermochemical Aspects of Combustion, WILEY-VCH Verlag GmbH & Co. KG, Weinheim, 2007, pp. 69-112.
[26] Servicio de Criminalística de la Guardia Civil (SECRIM), Explosives and standard samples, Guardia Civil, 2015.
[27] J.M. Amigo, Practical issues of hyperspectral imaging analysis of solid dosage forms, Analytical and Bioanalytical Chemistry 398(1) (2010) 93--109.
[28] M. Vidal, J.M. Amigo, Pre-processing of hyperspectral images. Essential steps before image analysis, Chemometrics and Intelligent Laboratory Systems 117 (2012) 138--148.
[29] D. Ballabio, Classification toolbox for MATLAB, 2016. http://michem.disat.unimib.it/chm/download/softwares.htm. 2016).
[30] D. Ballabio, V. Consonni, Classification tools in chemistry. Part 1: Linear models. PLS-DA, Analytical Methods (5) (2013) 3790-3798.

[31] J. Burger, P. Geladi, Hyperspectral NIR image regression part I: Calibration and correction, Journal of Chemometrics 19 (2005) 355–363.
[32] J.M. Amigo, C. Ravn, N.B. Gallagherd, R. Bro, A comparison of a common approach to partial least squares-discriminant analysis and classical least squares in hyperspectral imaging, International Journal of Pharmaceutics 373(1-2) (2009) 179--182.
[33] M.Á. Fernández de la Ossa, C. García-Ruiz, J.M. Amigo, Near promising future of near infrared hyperspectral imaging in forensic sciences, N I R News 25(4) (2014) 6--9.
[34] J.M. Amigo, J. Cruz, M. Bautista, S. Maspoch, J. Coello, M. Blanco, Study of pharmaceutical samples by NIR chemical-image and multivariate analysis, Trends in Analytical Chemistry 27(8) (2008) 696--713.
[35] J.M. Amigo Rubio, I. Martí, A. Gowen, Hyperspectral Imaging and Chemometrics: A Perfect Combination for the Analysis of Food Structure, Composition and Quality, in: F. Marini (Ed.), Data Handling in Science and Technology. Chemometrics in Food Chemistry, Elsevier, The Netherlands, 2013, pp. 343-370.
[36] J. Ferré Baldrich, Regression Diagnostics, in: S.D. Brown, R. Tauler, B. Walczak (Eds.), Comprehensive Chemometrics - Chemical and Biochemical Data Analysis, Elsevier2009, pp. 33-88.
[37] R. Tauler, M. Maeder, Two-Way Data Analysis: Multivariate Curve Resolution – Error in Curve Resolution, in: S.D. Brown, R. Tauler, B. Walczak (Eds.), Comprehensive Chemometrics - Chemical and Biochemical Data Analysis, Elsevier2009, pp. 325-342.
[38] F. Raposo, Evaluation of analytical calibration based on least-squares linear regression for instrumental techniques: A tutorial review, Trends in Analytical Chemistry (77) (2016) 167–185.
[39] J.H. Kalivas, Calibration Methodologies, in: S.D. Brown, R. Tauler, B. Walczak (Eds.), Comprehensive Chemometrics - Chemical and Biochemical Data Analysis, Elsevier2009, pp. 1-31.
[40] P.D. Wentzell, Other Topics in Soft-Modeling: Maximum Likelihood-Based Soft-Modeling Methods, in: S.D. Brown, R. Tauler, B. Walczak (Eds.), Comprehensive Chemometrics - Chemical and Biochemical Data Analysis, Elsevier2009, pp. 507-558.
[41] S.C. Rutan, A. de Juan, R. Tauler, Introduction to Multivariate Curve Resolution, in: S.D. Brown, R. Tauler, B. Walczak (Eds.), Comprehensive Chemometrics - Chemical and Biochemical Data Analysis, Elsevier2009, pp. 249-257.
[42] C. Ravn, E. Skibsted, R. Bro, Near-infrared chemical imaging (NIR-CI) on pharmaceutical solid dosage forms - Comparing common calibration approaches., Journal of Pharmaceutical and Biomedical Analysis 48 (2008) 554–561.
[43] R. Tauler, M. Maeder, A. De Juan, Multiset Data Analysis: Extended Multivariate Curve Resolution, in: S.D. Brown, R. Tauler, B. Walczak (Eds.), Comprehensive Chemometrics - Chemical and Biochemical Data Analysis, Elsevier2009, pp. 473-503.
[44] H.M. Heise, R. Winzen, Chemometrics in Near-Infrared Spectroscopy, in: H.W. Siesler, Y. Ozaki, S. Kawata, H.M. Heise (Eds.), Near-In frared Spectroscopy : Principles, Instruments, Applications, Wiley-VCH, Weinheim, 2002, pp. 125-162.
[45] Z. Abrego, N. Grijalba, N. Unceta, M. Maguregui, A. Sanchez, A. Fernández-Isla, M.A. Goicolea, R.J. Barrio, A novel method for the identification of inorganic and organic gunshot residue particles of lead-free ammunitions from the hands of shooters using scanning laser ablation-ICPMS and Raman micro-spectroscopy, Analyst 139(23) (2014) 6232-6241.

Figure 1. CLS results showing the GSR patterns of (A) S&B and (B) Sintox ammunition shot on white-cotton-fabric targets at 10 cm. Each target, which is the same in all horizontal images, was matched against the white, black or white-stamped cotton fabrics working as standards' spectra, placed at

the bottom row (C). Relative weight and density are the quantitative values indicated inside parenthesis.

Figure 2. CLS results showing the GSR patterns in white- and black-cotton fabrics shot at 10 cm with either S&B or Sintox ammunitions when targets were matched against both propellants' spectra and the corresponding target's spectrum. A) White-cotton-fabric shot with S&B; B) White-cotton-fabric shot with Sintox; C) Black-cotton-fabric shot with S&B; and D) Black-cotton-fabric shot with Sintox. Relative weight and density are the quantitative values indicated into parenthesis.

Figure 3. CLS results showing the GSR patterns in white- and black-cotton fabrics shot at 10 cm with either S&B or Sintox ammunitions when targets were matched against the spectra of the pure standards. The cotton-fabrics, cellulose, and the ammunition standards were kept out in order to keep the images as uncrowded as possible. A) White-cotton-fabric shot with S&B; B) White-cotton-fabric shot with Sintox; C) Black-cotton-fabric shot with S&B; and D) Black-cotton-fabric shot with Sintox. Relative weight and density are the quantitative values indicated into parenthesis.

Supplemental Figure 1. Left: S&B and Sintox ammunition propellant spectra sets used for the matching in the entire propellant-based approach. The median spectra (in orange) are shown only as visual references, since they were not used for any matching. Right: The most abundant spectra detected in the propellant's standards by the CLS models.

Highlights

- The use of chemical imaging in the SWIR region for analysing gunshot residues patterns in cotton-fabric targets shot with conventional and non-toxic ammunition.
- A non-destructive, non-toxic, rather fast, visual and HSI-based approach based on classical least squares regression, and tested with the ammunition propellants and their components' spectra.
- Nitrocellulose resulted an excellent standard for identifying GSR patterns; likewise, the propellants' spectra were satisfactorily used irrespective of the type of ammunition shot.
- The propellants' stabilizers, and its nitrated derivatives as well as DNT, could be recommended as complementary standards for confirming the GSR identification.
- This approach can be an alternative to the current and traditional chemical methods, based in presumptive and invasive colour tests.